

# Chemical Science

Accepted Manuscript



This is an *Accepted Manuscript*, which has been through the Royal Society of Chemistry peer review process and has been accepted for publication.

*Accepted Manuscripts* are published online shortly after acceptance, before technical editing, formatting and proof reading. Using this free service, authors can make their results available to the community, in citable form, before we publish the edited article. We will replace this *Accepted Manuscript* with the edited and formatted *Advance Article* as soon as it is available.

You can find more information about *Accepted Manuscripts* in the [Information for Authors](#).

Please note that technical editing may introduce minor changes to the text and/or graphics, which may alter content. The journal's standard [Terms & Conditions](#) and the [Ethical guidelines](#) still apply. In no event shall the Royal Society of Chemistry be held responsible for any errors or omissions in this *Accepted Manuscript* or any consequences arising from the use of any information it contains.



## Chemical Science

## ARTICLE

# Metal-Organic Framework-Based CoP/Reduced Graphene Oxide: High-Performance Bifunctional Electrocatalyst for Overall Water Splitting

Received 00th January 20xx,  
Accepted 00th January 20xx

DOI: 10.1039/x0xx00000x

www.rsc.org/

Long Jiao, Yu-Xiao Zhou and Hai-Long Jiang\*

The efficient and cost-effective electrocatalysts for hydrogen evolution reaction (HER) and oxygen evolution reaction (OER), especially bifunctional catalysts for overall water splitting, are highly desired. In this work, with rationally designed sandwich-type metal-organic framework/graphene oxide as a template and precursor, layered CoP/reduced graphene oxide (rGO) composite has been successfully prepared via pyrolysis and subsequent phosphating process. The resultant CoP/rGO-400 exhibits excellent HER activity in acid solution. More importantly, the catalyst manifests excellent catalytic performances for both HER and OER in basic solution. Therefore, it can be utilized as a bifunctional catalyst on both anode and cathode for overall water splitting in basic media, even displaying superior activity to that of the integrated Pt/C and IrO<sub>2</sub> catalyst couple.

## Introduction

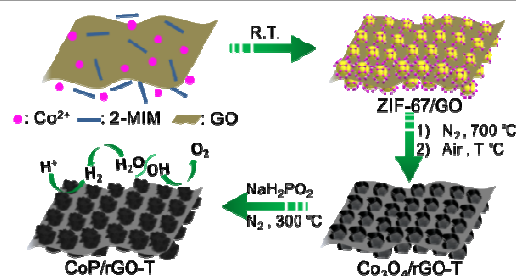
With increasing environmental concerns and consumption of fossil fuel, there is an urgent demand to develop alternative clean energy, such as, hydrogen. Electrocatalytic water splitting, a combination of hydrogen evolution reaction (HER) and oxygen evolution reaction (OER) to generate hydrogen and oxygen, respectively, has been recognized to be one of the most promising ways for energy conversion.<sup>1</sup> To reach this goal, the development of efficient catalysts to accelerate the kinetics of both half-cell reactions is a prerequisite.<sup>1</sup> Precious metals (Pt) and noble metal oxides (RuO<sub>2</sub>, IrO<sub>2</sub>) possess the best activity for HER and OER, respectively, while their large-scale industrial application is impeded by the high cost and scarcity.<sup>1b,f</sup> It is highly desirable to develop cost-effective catalysts with high activity and durability. Currently, much effort was devoted to the exploration of the half-cell reactions and great progress has been achieved, for examples, transition-metal sulfides, selenides, carbides and phosphides exhibit stable catalytic activity for HER in acid solution,<sup>2</sup> and transition metal oxides/hydroxides are found to be active for more challenging OER in basic solution.<sup>3</sup> To meet the practical application, the HER and OER should be conducted in the same electrolyte based on a single catalyst to achieve overall water splitting. However, the current prevailing water splitting

requires the integration of two types of catalysts that are specially suitable for HER and OER, respectively. Such combination is usually incompatible and thus results in poor overall performance. Therefore, the development of bifunctional catalysts, highly active for both HER and OER, is of prime importance for overall water splitting, while remains a significant challenge and has been rarely reported thus far.<sup>1f,g,4</sup>

To achieve high catalytic activity, nanostructuring the catalysts with porous character would be an essential way to expose active sites as far as possible to the electrolyte and substrate. In this context, metal-organic frameworks (MOFs), a family of crystalline porous materials with well-organized structures, should be ideal precursors.<sup>5</sup> Recently, MOFs as templates/precursors have been demonstrated to afford various porous nanostructured carbon/metal oxides with good catalytic performance.<sup>6,7</sup> Despite this, the poor electrical conductivity of MOF-derived nanocomposites is unfavorable for the electrocatalysis. Given that graphene oxide (GO) has been well documented to be an excellent conductor, the formation of hybrid structures between MOF-derived nanocomposites and GO might effectively exert their

Hefei National Laboratory for Physical Sciences at the Microscale, Key Laboratory of Soft Matter Chemistry, Chinese Academy of Sciences, Collaborative Innovation Center of Suzhou Nano Science and Technology, Department of Chemistry, University of Science and Technology of China, Hefei, Anhui 230026 (P.R. China)  
E-mail: jianglab@ustc.edu.cn

† Electronic Supplementary Information (ESI) available: Preparation of graphene oxide (GO), figures referred in the text and comparison of the literature catalytic parameters of various non-noble electrocatalysts. See DOI: 10.1039/x0xx00000x



**Scheme 1** Illustration of the fabrication procedure for CoP/rGO-T nanocomposite.

synergistic effect by taking advantage of their respective advantages.<sup>7</sup>

Among different electrocatalysts for HER or OER, transition metal phosphides (TMP) are very promising not only because of their high abundance and low cost but also owing to the great acid-base stability in the pH range of 0-14. In this work, we have fabricated a MOF/GO sandwich-type composite with sheet-like structure based on the template role of GO via a facile one-step room-temperature reaction, without any bridging agent. Upon pyrolysis, the Co-based MOF/GO was converted to porous Co<sub>3</sub>O<sub>4</sub>/rGO, which was further phosphated to afford porous CoP/rGO nanocomposite with retained sheet-like morphology (Scheme 1). The MOF-derived porous crystalline CoP nanostructure guarantees the highly exposed active sites, and the close contact between CoP and rGO contributes to a consecutive conductive network, which is crucial for electron transfer. As a result, the CoP/rGO nanocomposite exhibits excellent HER activity in a wide pH range of 0-14 with overpotentials of 105 mV in acid solution and 150 mV in basic solution at 10 mA/cm<sup>2</sup>. In addition, it also displays outstanding OER activity in basic solution with an overpotential of 340 mV at 10 mA/cm<sup>2</sup>. When CoP/rGO was employed as a bifunctional catalyst in both anode and cathode, overall water splitting in basic solution has been achieved with high efficiency, which is even superior to the integrated Pt/C and IrO<sub>2</sub> catalyst couple.

## Experimental

### Materials and Instrumentation

All chemicals were from commercial and used without further purification. Deionized water with the specific resistance of 18.2 MΩ·cm was obtained by reversed osmosis followed by ion-exchange and filtration.

Powder X-ray diffraction (XRD) studies were carried out on a Japan Rigaku SmartLab<sup>TM</sup> rotation anode X-ray diffractometer equipped or Holland X'Pert PRO fixed anode X-ray diffractometer equipped with graphite monochromatized Cu Kα radiation (λ = 1.54 Å). Field-emission scanning electron microscopy (FE-SEM) was carried out with a field emission scanning electron microanalyzer (Zeiss Supra 40 scanning electron microscope at an acceleration voltage of 5 kV). The transmission electron microscopy (TEM) and high-resolution TEM were acquired on JEOL-2100F with an electron acceleration energy of 200 kV. The content of nitrogen was measured by using a VarioELIII Elemental analyzer. The X-ray photoelectron spectroscopy (XPS) measurements were performed by using an ESCALAB 250Xi high-performance electron spectrometer using monochromatized Al Kα (hν = 1486.7 eV) as the excitation source. The nitrogen sorption isotherms were measured by using an automatic volumetric adsorption equipment (Micromeritics ASAP 2020). Prior to nitrogen adsorption/desorption measurement, the samples were dried overnight at 150 °C under vacuum.

### Synthesis

**Preparation of Co<sub>3</sub>O<sub>4</sub>/rGO-400:** The Co(NO<sub>3</sub>)<sub>2</sub>·6H<sub>2</sub>O (383 mg) was

dispersed in a mixture solution A with 15 mL methanol and 15 ml ethanol, and 2-methylimidazole (410 mg) was dispersed in a mixture solution B with 5 mL methanol and 5 ml ethanol solution. The GO solution (7.5 mg, 5 mg/mL) was added into the mixture solution A dropwise under vigorous stirring, followed by introducing the solution B and the mixed solution was stirred for another 5 min. Then the mixture was kept undisturbed at room temperature for 24 h. The product was obtained by suction filtration and washing with water at least three times. After freeze drying, the purple powder was obtained and heated at 700 °C for 10 min at a heating rate of 5 °C/min under N<sub>2</sub> atmosphere and then in air at 400 °C for another 2 h to afford Co<sub>3</sub>O<sub>4</sub>/rGO-400. For comparison, Co<sub>3</sub>O<sub>4</sub>/rGO-350 and Co<sub>3</sub>O<sub>4</sub>/rGO-450 were also synthesized via a similar procedure, except for the calcination temperature in air being changed to 350 and 450 °C, respectively.

**Preparation of CoP/rGO-400:** The Co<sub>3</sub>O<sub>4</sub>/rGO-400 composite (10 mg) and NaH<sub>2</sub>PO<sub>2</sub> (100 mg) were put at two separate positions in a porcelain boat and charged into a tube furnace with NaH<sub>2</sub>PO<sub>2</sub> at the upstream side of the furnace. The furnace was allowed to heat at 300 °C for 2 h with a heating speed of 2 °C/min. Next, the impurities and unstable composition were removed by soaking the sample in HCl (2M) followed by thorough rinsing to yield CoP/rGO-400. The CoP/rGO-350 and CoP/rGO-450 were also obtained by the same phosphating treatment starting from Co<sub>3</sub>O<sub>4</sub>/rGO-350 and Co<sub>3</sub>O<sub>4</sub>/rGO-450, respectively.

**Preparation of CoP-400:** The CoP-400 was synthesized via the same method as that for CoP/rGO-400 without adding GO solution.

**Preparation of rGO:** The graphene oxide (20 mg) obtained by freeze drying was treated by the same process as that for CoP/rGO-400.

### Electrochemical measurements

Electrochemical measurements were performed with a CHI 760E electrochemical analyzer (CH Instruments, Inc., Shanghai) and a rotating disk electrode (RDE) (Pine Instruments, Grove city, PA) with a speed of 1600rpm. All electrochemical measurements were conducted in a typical three-electrode setup with a Pt counter electrode and Ag/AgCl reference electrodes. The 0.5M H<sub>2</sub>SO<sub>4</sub> solution and 1M KOH solution were used for electrochemical measurements and the solutions were purged with N<sub>2</sub> for 30 min HER or overall water splitting test or with O<sub>2</sub> prior to OER test. Before recording the electrochemical activity of catalyst, the catalyst was activated by 20 cyclic voltammetry scans at a scan rate of 100 mV/s. LSV measurements were conducted with scan rate of 5 mV/s. All potentials reported in this paper were converted from vs Ag/AgCl to vs RHE by adding a value of 0.197 + 0.059 × pH. All data are presented without iR compensation.

The catalyst ink was prepared by dispersing 2 mg of catalyst into 1 mL of ethanol solvent containing 10 μL of 5 wt% Nafion and sonicated for 30 min. Then 28 μL of the catalyst ink was loaded onto a GCE of 5 mm diameter (loading amount: ~ 0.28 mg/cm<sup>2</sup>).

To evaluate the bifunctionality of CoP/rGO in alkaline solutions, the catalyst was also loaded on two 1\*1 cm carbon fiber paper (loading amount:  $\sim 0.28 \text{ mg/cm}^2$ ).

## Results and discussion

The zeolite-type MOF,  $\text{Co}(\text{2-MIM})_2$  (called ZIF-67, 2-MIM = 2-methylimidazole),<sup>8</sup> featuring a three-dimensional (3D) network with 1.1 nm cages and a large surface area (BET,  $>1500 \text{ m}^2/\text{g}$ ), is very suitable for acting as a template/precursor and can be converted to Co or  $\text{CoO}_x$ -based composite upon pyrolysis.<sup>9</sup> The introduction of GO template into the growth solution for ZIF-67 in mixed solvents leads to the successful fabrication of ZIF-67/GO with inherited sheet-like morphology of GO. It is clearly visible that ZIF-67 particles in 100~200 nm size are grown on the both surfaces of GO to give a sandwich-type structure, clearly demonstrating the template role of GO. The thickness of the ZIF-67/GO layer with rough surfaces is 200-400 nm and the successful synthesis of ZIF-67 is supported by powder X-ray diffraction (XRD) pattern (Fig. 1a, S1†). It is noteworthy that, although a few MOF-GO composites have been synthesized by direct growth of MOF in the presence of GO, no sheet-like morphology was reported for their resultant products;<sup>7a,10</sup> or ZIF-8/GO layered structure can be obtained only in the presence of PVP as an additional binder.<sup>7c</sup> This is a very rare synthesis of MOF/GO sheets based on GO template without any bridging agent.

The ZIF-67/GO underwent pyrolysis at 700 °C in  $\text{N}_2$  atmosphere and subsequent oxidation at different temperatures to afford  $\text{Co}_3\text{O}_4/\text{rGO-T}$  (T represents oxidation temperature) with retained layered structure (Fig. S2†), the BET surface area of which reached to  $40 \text{ m}^2/\text{g}$ , thanks to the high porosity of ZIF-67 (Fig. S3, S4†). Upon further phosphating process for the cobalt oxide, CoP/rGO-T (T = 350, 400, 450) were obtained and the presence of CoP species was approved by powder XRD profiles (Fig. S5†). As a representative, the resultant CoP/rGO-400 has been found to mostly maintain the

sheet-like morphology (Fig. 1b, S6†), although the thickness shrinks to  $\sim 200 \text{ nm}$  due to the removal of organic species during the heat treatment. As expected, the CoP/rGO-400 exhibits porous character and possesses hierarchical pores, especially macropores (Fig. S7†), in good agreement with the TEM result (Fig. 1c). The high-resolution TEM (HRTEM) image reveals clear lattice fringes with interplanar spacing of 0.19 nm corresponding to the (211) planes of CoP, further manifesting the formation of crystalline CoP species. In addition, the selected area electron diffraction (SAED) pattern exhibits the individual spots associated with concentric rings indexed to the (011), (111), (211) and (301) planes of orthorhombic CoP (Fig. 1d).<sup>2f,11</sup> The GO was reduced during the thermal treatment, as indicated by the weakened intensity of oxygen-containing bonds in the X-ray photoelectron spectroscopy (XPS) survey (Fig. S8†).

To evaluate the electrocatalytic HER activity, the catalysts were deposited on the RDE with a fixed mass loading ( $\sim 0.28 \text{ mg/cm}^2$ ). The HER performances were measured in acid (0.5M  $\text{H}_2\text{SO}_4$ ) and alkaline (1M KOH) solutions, respectively (Fig. 2). Bare GCE, rGO, CoP and commercial Pt/C (20 wt%) were also examined for comparison. As expected, Pt/C shows the most excellent activity while bare GCE and rGO have very poor HER performances. Surprisingly, the ZIF-67-derived CoP exhibits very high activity and the CoP/rGO-400 is more active, possibly due to the synergistic effect between the porous CoP and conductive rGO, the latter of which significantly lowers the impedance of CoP/rGO-400 (Fig. S9†). As determined from linear sweep voltammetry (LSV) in acid solution (Fig. 2a), the HER onset potential of CoP/rGO-400 is  $\sim 13 \text{ mV}$  and the kinetic current density reaches to  $10 \text{ mA/cm}^2$  at an overpotential of 105 mV. The corresponding Tafel slope is 50 mV/dec (Fig. 2c). The very low overpotential and Tafel slope indicate a higher HER activity than almost all state-of-the-art HER catalysts in acid solution, upon considering the same catalyst loading (Table S1†).<sup>12</sup> Moreover, its polarization curve after 3000 cycles of continuous CV scanning shows negligible difference with the initial one in 0.5M  $\text{H}_2\text{SO}_4$  (Fig. 2e). The chronoamperometry test for CoP/rGO-400 at an overpotential of 105 mV suggests that the activity remains very well even after 80000 seconds (Fig. 2e, inset). In addition, similar results have been obtained when CoP/rGO-400 was applied in alkaline condition. It exhibits a low overpotential of 150 mV at  $10 \text{ mA/cm}^2$ , superior to those of CoP, rGO and bare GCE (Fig. 2b), and a Tafel slope of 38 mV/dec comparable to that of Pt/C (Fig. 2d). These values are much lower than those used by other base metal HER catalysts in basic media (Table S2†). There is only a slight activity loss after 3000 cycles, while the chronoamperometry test for 80000 seconds presents its reliable stability at an overpotential of 150 mV (Fig. 2f). It is noteworthy that although Pt/C shows a very small onset potential, the catalytic current density of CoP/rGO-400 surpasses that of Pt/C when the overpotential exceeds 240 mV in alkaline solution. Taken together, the CoP/rGO-400 shows excellent HER activity and durability in both acidic and alkaline solutions.

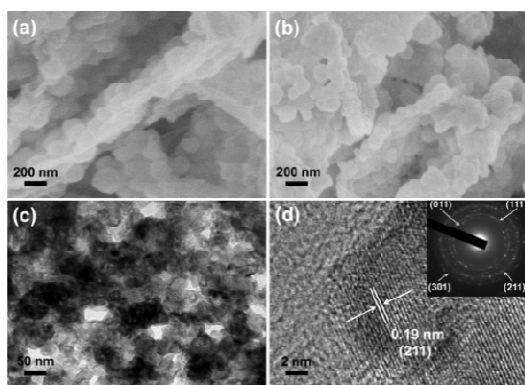


**Fig. 1** Scanning electron microscope (SEM) images of (a) ZIF-67/GO and (b) CoP/rGO-400. (c) Transmission electron microscopy (TEM) and (d) high-resolution TEM images of CoP/rGO-400 (Inset in d: SAED for CoP nanocrystal).



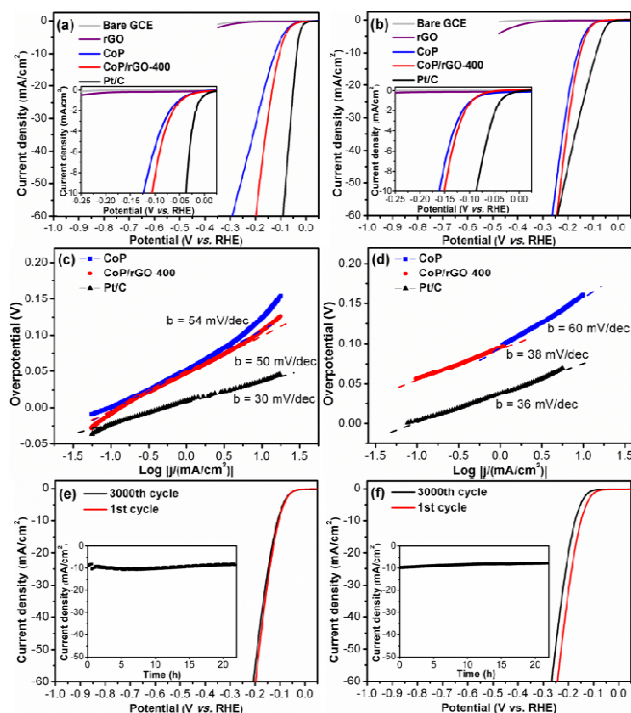


**Fig. 2** Electrochemical HER activity of CoP/rGO-400. (a) LSV curves, (c) Tafel slopes and (e) durability test in 0.5M H<sub>2</sub>SO<sub>4</sub> solution; (b) LSV curves, (d) Tafel slopes and (f) durability test in 1M KOH solution (insets in e and f: Time-dependent current density curves under static overpotentials of 105 mV in 0.5M H<sub>2</sub>SO<sub>4</sub> and 150 mV in 1M KOH solution, respectively).

It is even more challenging to obtain an efficient catalyst for OER as it is a very complex and energy-intensive process, in which the O-H bond breaking and O=O bond formation as well as the four-electron transfer process is a sluggish kinetics.<sup>1c,e</sup> It has been reported that CoP can act as OER catalyst via in-situ transformation very recently.<sup>4b,13</sup> Therefore, the OER performance of CoP/rGO-400 was investigated in 1M KOH solution. Delightfully, CoP/rGO-400 can reach a current density of 10 mA/cm<sup>2</sup> at an overpotential of 340 mV with a Tafel slope of 66 mV/dec, which are superior to CoP, rGO and even IrO<sub>2</sub>, the state-of-the-art OER catalyst (Fig. 3a, b). The durability test indicates that although there is a little regression after 3000 cycles, CoP/rGO-400 is pretty stable at an overpotential of 340 mV for 80000 s and remains a very high activity (Fig. 3c). Control experiments for CoP/rGO-T catalysts prepared at different oxidation temperatures have suggested the best electrochemical performances of CoP/rGO-400 for both HER and OER (Fig. S10–12<sup>†</sup>). The XPS spectra for CoP/rGO-400 after OER test clearly demonstrate the negligible incorporation of Fe species into the catalyst during OER reaction in KOH solution, different from the recent report (Fig. S13<sup>†</sup>).<sup>14</sup> In addition, given that Co<sub>3</sub>O<sub>4</sub>/rGO-400 is electrochemically active in alkaline solution, the comparison between CoP/rGO-400 and Co<sub>3</sub>O<sub>4</sub>/rGO-400 has been made and the result shows that CoP/rGO-400 is much more active than Co<sub>3</sub>O<sub>4</sub>/rGO-400 for HER and OER in 1M KOH (Fig. S14<sup>†</sup>).

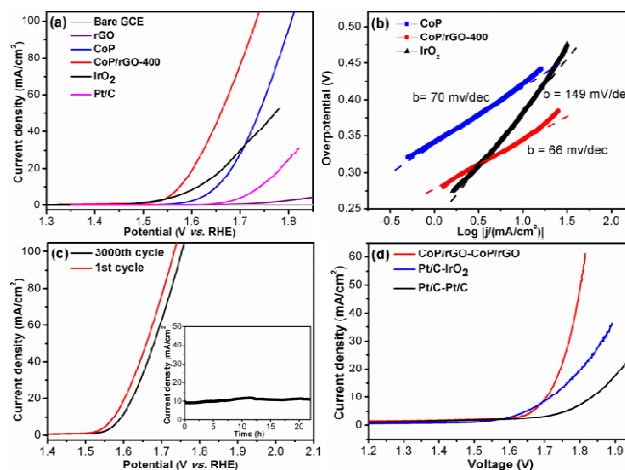


**Fig. 3** (a) LSV curves, (b) Tafel slopes, and (c) durability test for electrochemical OER of CoP/rGO-400 (Inset: Time-dependent current density curve of CoP/rGO-400 under static overpotential of 340 mV in 1M KOH solution). (d) Bifunctional water electrolysis tested by LSV in 1M KOH solution.

To probe the composition change of CoP/rGO-400 after HER and OER, high-resolution XPS spectra for as-prepared, post-HER and post-OER catalysts were collected. For the as-prepared catalyst, the Co 2p spectra show two peaks at 793.4 and 778.4 eV, corresponding to Co 2p<sub>3/2</sub> and Co 2p<sub>1/2</sub> of metallic Co, respectively (Fig. S15a<sup>†</sup>);<sup>15</sup> the P 2p spectra display two peaks at 129.4 eV and 130.2 eV related to the signals of phosphide, while the peak at 133.6 eV gradually decreasing along with Ar<sup>+</sup> sputtering should be attributed to superficial oxidation of CoP (Fig. S15b<sup>†</sup>).<sup>15,16</sup> The peaks of Co 2p for post-HER catalyst are similar to those of the as-prepared one, implying the retained metallic Co during HER (Fig. S15c<sup>†</sup>). Interestingly, only the peak at 129.9 eV is observable while the phosphate peak at 133.6 eV is absent from the P 2p spectra of the post-HER sample, possibly due to the dissolution of cobalt phosphate under cathodic condition (Fig. S15d<sup>†</sup>).

In comparison, besides the metallic Co 2p peaks at 778.4 and 793.4 eV, two new peaks at 781.4 and 797.0 eV, as well as their satellite peaks at 786.8 and 803.6 eV, emerge in the Co 2p spectra for post-OER catalyst and those can be assigned to Co<sub>3</sub>O<sub>4</sub> (Fig. S15e<sup>†</sup>).<sup>4b</sup> The P 2p spectra also show a phosphate peak at 133.4 eV, together with the phosphide feature at 129.5 eV (Fig. S15f<sup>†</sup>). Different from that in as-prepared CoP/rGO-400, the peaks for Co<sub>3</sub>O<sub>4</sub> and phosphate in post-OER catalyst remain strong even after long-time Ar<sup>+</sup> sputtering, indicating that CoP in the catalyst is partially oxidized to Co<sub>3</sub>O<sub>4</sub> and cobalt phosphate during OER. Such in-situ transformation explains the excellent OER activity of CoP/rGO-400 and that is in accordance with the reported results.<sup>4b,13</sup>

Encouraged by the above results, a two-electrode configuration was employed with CoP/rGO-400 as a bifunctional electrocatalyst to investigate its performance for overall water splitting. Since Pt/C is well-established for HER and IrO<sub>2</sub> for OER, the integration of Pt/C and IrO<sub>2</sub> couple would

**Table 1** Comparison of catalytic results for overall water splitting in 1M KOH solution.

HER <sub>catalyst</sub>	OER <sub>catalyst</sub>	E <sub>HER</sub> <sup>a</sup>	E <sub>OER</sub> <sup>b</sup>	E (V) <sup>c</sup>
Pt/C	Pt/C	-90	1742	1.83
Pt/C	IrO <sub>2</sub>	-90	1625	1.71
CoP/rGO-400	CoP/GO-400	-150	1570	1.70

Potentials for <sup>a</sup>HER (unit: mV), <sup>b</sup>OER (unit: mV) and <sup>c</sup>overall water splitting at current density of 10 mA/cm<sup>2</sup>.

provide a superb catalytic system, which, indeed, realizes water splitting with an overpotential of 480 mV at 10 mA/cm<sup>2</sup> and a Tafel slope of 201 mV/dec. When Pt/C was used as both electrodes, much reduced catalytic performance was obtained (overpotential of 600 mV at 10 mA/cm<sup>2</sup> and a Tafel slope of 251 mV/dec). In stark contrast, CoP/GO-400, being applied as both electrodes, outperforms the both systems and affords an overpotential of 470 mV at 10 mA/cm<sup>2</sup> and a Tafel slope of 135 mV/dec (Fig. 3d, S16<sup>†</sup>). Particularly, the H<sub>2</sub> and O<sub>2</sub> yields during water splitting over CoP/GO-400 were measured and the obtained molar ratio of H<sub>2</sub>/O<sub>2</sub> fits well with 2:1 and the total yield fits 100% Faradaic efficiency (Fig. S17<sup>†</sup>). The separated HER and OER as well as overall water splitting performances of CoP/rGO-400, compared with Pt/C, IrO<sub>2</sub> and their integrated couples, are shown in Table 1, clearly presenting the superb electrocatalytic activity of CoP/rGO-400.

It should be noted that Sun et al. reported HER catalysts derived from ZIF-67 during the submission of our work.<sup>17</sup> Apparent advantages of our work have been found after careful investigation into their work and the results reported herein. The detailed comparison are listed as follows: 1) For catalysis, to clarify the real active site, phase pure catalyst is highly desired unless one can demonstrate that a mixture possesses obvious advantages. The catalysts reported by Sun et al. are a mixture of CoP and Co<sub>2</sub>P, while no pure CoP or Co<sub>2</sub>P was obtained in their work. In contrast, pure CoP was obtained as active site in our work (Fig. S5<sup>†</sup>). 2) The heterogeneous nucleation/growth of ZIF-67 on substrate is very challenging as the nucleation of ZIF-67 is very fast and it is prone to self-nucleation.<sup>18</sup> For the first time, we have successfully synthesized 2D ZIF-67/GO sheets with a sandwich-like morphology in the absence of binding agent via a facile room-temperature route (Scheme 1). Our success would offer important reference for the synthesis of other MOFs/GO composites. 3) To fabricate a highly active electrocatalyst, we have rationally combined ZIF-67 (as a porous CoP precursor) and GO (as a 2D hard template) to give 2D ZIF/GO sheets and the derived CoP/rGO-400 composite (Fig. 1a). As a result, with the help of GO, the conductivity and electrochemical activity of CoP/rGO-400 is much better than pure CoP, which fits well with our original expectation. Compared to our rational design and synthesis, Sun et al. just worked on the thermal conversion of single ZIF-67 to Co-P mixture species. 4) Thanks to the rational design, the resultant CoP/rGO-400 catalyst exhibits superb HER and OER activity in 1M KOH with an overpotential of 150 mV and 340 mV, respectively, at a mass loading of 0.28 mg/cm<sup>2</sup> (Fig. 2b, 3a). In contrast, sun's work is

about 180 mV and 350 mV at 0.283 mg/cm<sup>2</sup>. Note that both HER and OER activities of CoP/rGO-400 increase along with increased mass loading (Fig. S18<sup>†</sup>). When the mass loading reached 0.42 mg/cm<sup>2</sup>, the overpotential of our CoP/rGO-400 for HER and OER in 1M KOH are 104 mV and 320 mV, respectively, which are even better than the result at 1 mg/cm<sup>2</sup> in Sun's work (154 mV for HER and 319 mV for OER). In our work, the H<sub>2</sub> and O<sub>2</sub> yields over time during overall water splitting have demonstrated that the molar ratio of H<sub>2</sub>/O<sub>2</sub> fits well with 2:1 and the total yield fits 100% Faradaic efficiency (Fig. S17<sup>†</sup>), while similar tests are lacking in Sun's report. On the whole, our work is significantly different from Sun's work, not only the idea of catalyst design, but also catalyst fabrication, main active sites/composition (CoP and Co<sub>2</sub>P mixture for Sun et al., while CoP only for us) as well as final catalytic performances.

## Conclusions

In summary, we have developed CoP/rGO layered composites as bifunctional catalysts for overall water splitting, via a GO-templated MOF growth and subsequent pyrolysis and phosphating process. The resultant CoP/rGO-400 nanocomposite exhibits superior HER catalytic performance in acid solution. Moreover, it is able to behave as an electrocatalyst for both HER and OER, in alkaline solution with great efficiency and durability. The excellent electrocatalytic performance might be attributed to the synergistic effect between MOF-derived CoP and rGO in terms of porous nanostructures, high electrical conductivity and stability against corrosion during HER and OER. Significantly, CoP/rGO-400 can be directly employed as catalysts for both electrodes to afford efficient H<sub>2</sub> and O<sub>2</sub> generation in a single electrolyzer, making it a promising overall water splitting catalyst. This study opens up an exciting avenue to the design of efficient electrocatalysts based on MOF-GO composites by integrating their respective merits. Given the huge diversity and tailorability of MOFs, the strategy presented herein holds great promise for electrocatalysis and studies along this line are ongoing in our laboratory.

## Acknowledgements

We are grateful to the reviewers for their insightful comments and valuable suggestions. This work is supported by the NSFC (21371162, 51301159 and 21521001), the 973 program (2014CB931803), the Recruitment Program of Global Youth Experts and the Fundamental Research Funds for the Central Universities (WK2060190026).

## Notes and references

- (a) J. Greeley, T. F. Jaramillo, J. Bonde, I. Chorkendorff and J. K. Nørskov, *Nat. Mater.*, 2006, **5**, 909; (b) H. B. Gray, *Nat. Chem.*, 2009, **1**, 7; (c) M. G. Walter, E. L. Warren, J. R. McKone, S. W. Boettcher, Q. Mi, E. A. Santori and N. S. Lewis, *Chem. Rev.*, 2010, **110**, 6446; (d) T. R. Cook, D. K. Dogutan, S.

- Y. Reece, Y. Surendranath, T. S. Teets and D. G. Nocera, *Chem. Rev.*, 2010, **110**, 6474; (e) R. Subbaraman, D. Tripkovic, K.-C. Chang, D. Strmcnik, A. P. Paulikas, P. Hirunsit, M. Chan, J. Greeley, V. Stamenkovic and N. M. Markovic, *Nat. Mater.*, 2012, **11**, 550; (f) Y. Yang, H. Fei, G. Ruan and J. M. Tour, *Adv. Mater.*, 2015, **27**, 3175; (g) H. Wang, H.-W. Lee, Y. Deng, Z. Lu, P.-C. Hsu, Y. Liu, D. Lin and Y. Cui, *Nat. Commun.*, 2015, **6**, 7261.
- 2 (a) T. F. Jaramillo, K. P. Jørgensen, J. Bonde, J. H. Nielsen, S. Horch and I. Chorkendorff, *Science*, 2007, **317**, 100; (b) Y. Li, H. Wang, L. Xie, Y. Liang, G. Hong and H. Dai, *J. Am. Chem. Soc.*, 2011, **133**, 7296; (c) C. G. Morales-Guio and X. Hu, *Acc. Chem. Res.*, 2014, **47**, 2671; (d) M.-R. Gao, J.-X. Liang, Y.-A. Cheng, Y.-F. Xu, J. Jiang, Q. Gao, J. Li and S.-H. Yu, *Nat. Commun.*, 2015, **6**, 5982; (e) L. Liao, S. Wang, J. Xiao, X. Bian, Y. Zhang, M. D. Scanlon, X. Hu, Y. Tang, B. Liu and H. H. Girault, *Energy Environ. Sci.*, 2014, **7**, 387; (f) Q. Liu, J. Tian, W. Cui, P. Jiang, N. Cheng, A. M. Asiri and X. Sun, *Angew. Chem. Int. Ed.*, 2014, **53**, 6710; (g) E. J. Popczun, C. G. Read, C. W. Roske, N. S. Lewis and R. E. Schaak, *Angew. Chem. Int. Ed.*, 2014, **53**, 5427; (h) D. Li, U. N. Maiti, J. Lim, D. S. Choi, W. J. Lee, Y. Oh, G. Y. Lee and S. O. Kim, *Nano Lett.*, 2014, **14**, 1228.
- 3 (a) T. Y. Ma, S. Dai, M. Jaroniec and S. Z. Qiao, *J. Am. Chem. Soc.*, 2014, **136**, 13925; (b) Z. Zhuang, W. Sheng and Y. Yan, *Adv. Mater.*, 2014, **26**, 3950; (c) H. Jin, J. Wang, D. Su, Z. Wei, Z. Pang and Y. Wang, *J. Am. Chem. Soc.*, 2015, **137**, 2688; (d) L. Wu, Q. Li, C. H. Wu, H. Zhu, A. Mendoza-Garcia, B. Shen, J. Guo and S. Sun, *J. Am. Chem. Soc.*, 2015, **137**, 7071.
- 4 (a) C. Tang, N. Cheng, Z. Pu, W. Xing and X. Sun, *Angew. Chem. Int. Ed.*, 2015, **54**, 9351; (b) N. Jiang, B. You, M. Sheng and Y. Sun, *Angew. Chem. Int. Ed.*, 2015, **54**, 6251; (c) Y.-P. Zhu, Y.-P. Liu, T.-Z. Ren and Y.-Z. Yong, *Adv. Funct. Mater.*, 2015, **25**, 7337.
- 5 (a) J. R. Long and O. M. Yaghi, *Chem. Soc. Rev.*, 2009, **38**, 1213; (b) H.-C. Zhou, J. R. Long and O. M. Yaghi, *Chem. Rev.*, 2012, **112**, 673; (c) H.-C. Zhou and S. Kitagawa, *Chem. Soc. Rev.*, 2014, **43**, 5415.
- 6 (a) S. Ma, G. A. Goenaga, A. V. Call and D.-J. Liu, *Chem. Eur. J.*, 2011, **17**, 2063; (b) W. Zhang, Z.-Y. Wu, H.-L. Jiang and S.-H. Yu, *J. Am. Chem. Soc.*, 2014, **136**, 14385; (c) Q. Lin, X. Bu, A. Kong, C. Mao, X. Zhao, F. Bu and P. Feng, *J. Am. Chem. Soc.*, 2015, **137**, 2235; (d) Y.-Z. Chen, C. Wang, Z.-Y. Wu, Y. Xiong, Q. Xu, S.-H. Yu and H.-L. Jiang, *Adv. Mater.*, 2015, **27**, 5010; (e) W. Xia, A. Mahmood, R. Zou and Q. Xu, *Energy Environ. Sci.*, 2015, **8**, 1837; (f) P. Zhang, F. Sun, Z. Xiang, Z. Shen, J. Yun and D. Cao, *Energy Environ. Sci.*, 2014, **7**, 442; (g) D. Zhao, J.-L. Shui, L. R. Grabstanowicz, C. Chen, S. M. Commet, T. Xu, J. Lu and D.-J. Liu, *Adv. Mater.*, 2014, **26**, 1093; (h) S. Zhao, H. Yin, L. Du, L. He, K. Zhao, L. Chang, G. Yin, H. Zhao, S. Liu and Z. Tang, *ACS Nano*, 2014, **8**, 12660.
- 7 (a) M. Jahan, Z. Liu and K. P. Loh, *Adv. Funct. Mater.*, 2013, **23**, 5363; (b) Y. Hou, T. Huang, Z. Wen, S. Mao, S. M. Cui and J. H. Chen, *Adv. Energy Mater.*, 2014, **4**, 1400337; (c) H.-X. Zhong, J. Wang, Y.-W. Zhang, W.-L. Xu, W. Xing, D. Xu, Y.-F. Zhang and X.-B. Zhang, *Angew. Chem. Int. Ed.*, 2014, **53**, 14235.
- 8 (a) R. Banerjee, A. Phan, B. Wang, C. Knobler, H. Furukawa, M. O'Keeffe and O. M. Yaghi, *Science*, 2008, **319**, 939; (b) J. Qian, F. Sun and L. Qin, *Mater. Lett.*, 2012, **82**, 220.
- 9 (a) R. Wu, X. Qian, X. Rui, H. Liu, B. Yadian, K. Zhou, J. Wei, Q. Yan, X.-Q. Feng, Y. Long, L. Wang and Y. Huang, *Small*, 2014, **10**, 1932; (b) N. L. Torad, M. Hu, S. Ishihara, H. Sukegawa, A. A. Belik, M. Imura, K. Ariga, Y. Sakka and Y. Yamauchi, *Small*, 2014, **10**, 2096; (c) Y.-X. Zhou, Y.-Z. Chen, L. Cao, J. Lu and H.-L. Jiang, *Chem. Commun.*, 2015, **51**, 8292; (d) W. Zhong, H. Liu, C. Bai, S. Liao and Y. Li, *ACS Catal.*, 2015, **5**, 1850; (e) H. Hu, B. Guan, B. Xia and X. W. Lou, *J. Am. Chem. Soc.*, 2015, **137**, 5590.
- 10 (a) B. C. Petit and T. J. Bandosz, *Adv. Mater.*, 2009, **21**, 4753; (b) M. Jahan, Q. Bao, J.-X. Yang and K. P. Loh, *J. Am. Chem. Soc.*, 2010, **132**, 14487; (c) C. Petit and T. J. Bandosz, *Adv. Funct. Mater.*, 2011, **21**, 2108; (d) J. H. Lee, S. Kang, J. Jaworski, K. Y. Kwon, M. L. Seo, J. Y. Lee and J. H. Jung, *Chem. Eur. J.*, 2012, **18**, 765.
- 11 Y. Li, M. A. Malik and P. O'Brien, *J. Am. Chem. Soc.*, 2005, **127**, 16020.
- 12 (a) Y. Yan, B. Xia, Z. Xu and X. Wang, *ACS Catal.*, 2014, **4**, 1693; (b) C. G. Morales-Guio, L. A. Stern and X. Hu, *Chem. Soc. Rev.*, 2014, **43**, 6555.
- 13 (a) J. Ryu, N. Jung, J. H. Jang, H. J. Kim and S. J. Yoo, *ACS Catal.*, 2015, **5**, 4066; (b) J. Chang, Y. Xiao, M. Xiao, J. Ge, C. Liu and W. Xing, *ACS Catal.*, 2015, **5**, 6874.
- 14 M. S. Burke, M. G. Kast, L. Trotochaud, A. M. Smith and S. W. Boettcher, *J. Am. Chem. Soc.*, 2015, **137**, 3638.
- 15 A. P. Grosvenor, S. D. Wik, R. G. Cavell and A. Mar, *Inorg. Chem.*, 2005, **44**, 8988.
- 16 F. H. Saadi, A. I. Carim, E. Verlage, J. C. Hemminger, N. S. Lewis and M. P. Soriaga, *J. Phys. Chem. C*, 2014, **118**, 29294.
- 17 B. You, N. Jiang, M. Sheng, S. Gul, J. Yano and Y. Sun, *Chem. Mater.*, 2015, **27**, 7636.
- 18 H. K. Kwon, H.-K. Jeong, A. S. Lee, H. S. An and J. S. Lee, *J. Am. Chem. Soc.*, 2015, **137**, 12304.